Received: 9 May 2019 | Revised: 6 March 2020 | Accepted: 9 March 2020

DOI: 10.1002/jbm.a.36937

Society For Biomaterials WILEY

ORIGINAL ARTICLE

Elastomeric polyurethane porous film functionalized with gastrodin for peripheral nerve regeneration

Qing Li[1] | Limei Li[1] | Mali Yu[1] | Meng Zheng[1] | Yao Li[2] | Jian Yang[3] | Min Dai[4] | Lianmei Zhong[5] | Lin Sun[6] | Di Lu[1]

[1]Science and Technology Achievement Incubation Center, Kunming Medical University, Kunming, China

[2]Department of Stomatology, The First People's Hospital of Yunnan Provience, Kunming, China

[3]Department of Biomedical Engineering, Materials Research Institute, The Huck Institutes of The Life Sciences, The Pennsylvania State University, University Park, Pennsylvania

[4]Department of Second Cardiology, The Third People's Hospital of Kunming, Kunming, China

[5]Department of Neurology, The First Affiliated Hospital, Kunming Medical University, Kunming, China

[6]Department of Cardiology, The Second Affiliated Hospital, Kunming Medical University, Kunming, China

Correspondence
Di Lu, Science and Technology Achievement Incubation Center, Kunming Medical University, Kunming 650500, China.
Email: ludi20040609@126.com

Lin Sun, Department of Cardiology, The Second Affiliated Hospital, Kunming Medical University, Kunming 650032, China.
Email: sunlinkm@sina.com

Funding information
Grants from Education Commission of Yunnan Province, Grant/Award Numbers: 2017zzx200, 2018Y046; International Science and Technology Cooperation Project of Yunnan Province, Grant/Award Number: 2018IA048; National Natural Science Foundation of China, Grant/Award Numbers: 81360200, 81460210, 81860326; Program for Innovative Research Team (in Science and Technology) in University of Yunnan Province.; Projects from the Department of Science and Technology of Yunnan Province, Grant/Award Numbers: 2017FA035, 2018FE001(-137), 2018FE001 (-165), 2019ZF011-2

Abstract

The extracellular matrix provides cells with a support structure and an attachment site in actual substrate. Its biochemical and surface properties play an important role in and have significant impact on cell attachment, proliferation, migration, differentiation, and gene expression. Leveraging the hydrophilicity and neuroprotective of gastrodin, a gastrodin/polyurethane (PU) elastomer was developed utilizing in situ polymerization and salt-leaching methods. The results showed that gastrodin/PU film had a good flexibility and supporting strength, as well as hydrophilicity. Thus film possessed highly surface area, interconnected porous structure with a pore size (10~60 μm) for cell attachment, and could provide surface cues to augment neurite extension. For PC12 cells cultured within the films, especially the 5gastrodin/PU group, presented a progressive increase with time, coupled with the upregulation of brain-derived neurotrophic factor and glial cell derived neurotrophic factor expression. This is the first report on the construction of a gastrodin/PU porous film, and the results reveal its promise as a scaffold material for neural tissue engineering.

KEYWORDS

gastrodin, hydrophilicity, mechanical properties, neurite extension, porous polyurethane

1 | INTRODUCTION

Peripheral nerve injury (PNI) is a very common clinical trauma, given a great number of patients suffering from varying degrees of paralysis or sensory deficits (Kehoe, Zhang, & Boyd, 2012; Shahriari et al., 2017; Vikström, Björkman, Carlsson, Olsson, & Rosén, 2018). Therefore, PNI has been the focus of many recent studies. Peripheral nerves have the ability to regenerate; however, regeneration must realize rapidly the functional recovery of both muscles and nerves. Currently, autologous graft serves as the gold standard in treating long nerve defects (Dixon et al., 2018; Vijayavenkataraman, Thaharah, Zhang, Lu, & Fuh, 2018); yet, associated problems include limited

Qing Li and Limei Li contributed equally to this work.

availability of donor source, the potential for undesirable neuroma formation, and microstructural mismatch (Chang et al., 2017; Chiono & Tonda-Turo, 2015; Gu, Ding, Yang, & Liu, 2011; Labroo et al., 2019). Hence, artificial nerve conduits, of which microenvironment can support neurogenesis, have been exploited as an alternative way to repair damaged nerve (Li et al., 2018; Wu et al., 2018). Nerve tissue scaffolds often seek to mimic natural microstructures with pore size ranging from 20 to 60 μm (Chiono & Tonda-Turo, 2015; Sridharan, Reilly, & Buckley, 2015), enabling the nutrient permeability along with available spaces for proper cellular network formation and inhibition of fibrous scar tissue invasion, as well as the biochemical composition of the extracellular matrix (ECM) in efforts to enhance nerve regeneration (Shahriari, Koffler, Tuszynski, Campana, & Sakamoto, 2017; Zhang et al., 2015). The nerve ECM is a hierarchical structure with nanofibrous featuring pores at the micrometer scale (Palumbo et al., 2002; Wang et al., 2010). Both the surface receptors and the functional cell domains are nanoscale, which facilitate cell–cell interactions (Hahm, 2014). Hence, ideally grafts with microstructures should mimic the structure of the natural ECM and further perform biological functions.

Manipulation of the microenvironment at the site of nerve repair to promote modulation of the host inflammatory response and cell migration and axon extension across the repair site is a challenge for functional improvement after grafting (Cattin et al., 2015; Mokarram, Merchant, Mukhatyar, Patel, & Bellamkonda, 2012). Addition of hydrophilic compositions has been widely investigated for not only improving the nutrient permeability but also reducing the inflammatory response (Nune, Krishnan, & Sethuraman, 2016). The hydrophilic/hydrophobic ratio can also influence cellular morphology and growth (Chang & Wang, 2011). Gastrodin is one of the active constituents isolated from the tuber of Gastrodia elata Blume (Tianma in Chinese), which is hydrophilic because of its polar hydroxyl moieties present in the side chain. Recent studies found that gastrodin has many biological functions, including anti-inflammatory (Peng et al., 2015; Wang et al., 2014), antioxidant (Peng et al., 2015), and anti-depressant (Wang et al., 2014) activity. Previous studies have reported that gastrodin is endowed with neuroprotective properties against hypoxia in the cultured cortical neurons (Xu, 2007) and supported the neuroprotective effects in mice (Peng et al., 2015). This together with the chemical nature and biological function of the grafts surface affects the protein adsorption; in turn, it regulates cell attachment, proliferation and elongation. Regarding the nature of gastrodin, it is critical to develop new scaffolds functionalized with gastrodin for manipulating cell behavior in neural tissue engineering.

Engineering scaffold plays an important role during tissue regeneration. Generally, scaffolds serve as an artificial ECM that establishes a template to support cells grow and maintain their differentiated functions, as well as guide the development of new tissue (Gu et al., 2011; Jeon et al., 2018). Biomimetic polymers such as chitosan (Manoukian, Arul, Rudraiah, Kalajzic, & Kumbar, 2019), gelatin (Farzamfar et al., 2019), collagen (Saeki et al., 2018), and hydrogel (Zou et al., 2018), have attracted great interest as scaffold biomaterials for neural tissue engineering due to their superior biological response. Presently, many studies have focused on designing scaffolds for neural tissue engineering, but many of them are unsatisfactory as they cannot meet all the requirements of a suitable environment for stem cell growth (Kehoe et al., 2012).

Polyurethane (PU) is an elastomer, whose advantages include good biocompatibility, biodegradability and mechanical properties, ease of processing, wide resource availability, as well as low cost (Uscátegui et al., 2019). PU has been designed into films, microspheres, nanoparticles, micelles, gels, fibers, and scaffolds for drug delivery and tissue engineering application (Chen et al., 2018; Shoaib, Ur Rahman, Saeed, & Naseer, 2018). Among these, the biodegradable PU with adequate biocompatibility and excellent mechanical qualities has been a choice for nerve graft material (Salehi et al., 2018). The PU scaffold can be structured with the hard/soft nanodomain on the nanoscale, the porous structure on the microscale (Princi, Vicini, Stagnaro, & Conzatti, 2011). The structures resemble segmented collagen, porous structure of natural nerve, which comprise the material basis of a high-performance scaffold for nerve regeneration (Arévalo, Uscategui, Diaz, Cobo, & Valero, 2016). Niu et al. have found that PU nerve conduit based on poly(ε-caprolactone) and poly(ethylene glycol) can promote peripheral nerve regeneration (Niu et al., 2014; Niu et al., 2015). The glial cells seeded onto PU/polylactide electrospun nonwovens also present good activity (Grzesiak et al., 2015). These studies supported the cytocompatibity of PU with glial cells. Besides, PU conduits showed no obvious fibrous capsules or other adverse reactions during a period of 6 months (Dezhznz, Xiao Hong, Yongnian, & Renji, 2007). However, the use of the PU based on gastrodin as a nerve biomaterial for peripheral nerve regeneration has not been attempted. We have studied the potential of gastrodin as an anti-inflammatory drug in neuropathological conditions (Dai et al., 2011), and developed a novel gastrodin-crosslinking PU elastomer in our lab (Li et al., 2018). Thus, we propose that PU functionalized with gastrodin can well fulfill the efficacy as a potential conduit material.

In this study, we engineered a porous film based on gastrodin and PU, to match with the multifunctional requirements for nerve reconstruction. It was surmised that gastrodin content alteration in the obtained films might affect the surface and mechanical properties, as well as guide the activity of PC12 cells adopted this study and the neurite extension. Differentiation of PC12 cells on the films was further examined by protein and gene analysis. A film with microstructure, good mechanical properties and hydrophilicity, effective neurite extension capacity would be a suitable candidate for nerve regeneration and functional recovery.

2 | MATERIALS AND METHODS

2.1 | Materials

Poly(ε-caprolactone)2000 (PCL2000), isophorone diisocyanate (IPDI) and lysine ethyl ester dihydrochlorid (Lys·OEt-2HCl)

were purchased from Aladdin Co. Ltd., China. Gastrodin (purity >99.0%) was purchased from Kunming Pharmaceutical Co. Ltd., China. The 1, 4-dioxane was purchased from Tianjin Fengchuan Chemical Reagent Technology (China). NaCl particles were ground into a fine powder and then sifted through sieves of 300 mesh diameter. The Dulbecco's modified Eagle's medium (DMEM) was purchased from HyClone. The fetal bovine serum (FBS) was obtained from Gibco. The cell counting kit-8 (CCK-8) assay was purchased from Dojindo Molecular Technologies, Japan. Live/dead reagent (Live/dead viability/cytotoxicity kit), TRIzol reagent (Ambion), and RevertAid First Strand cDNA Synthesis Kit were purchased from Thermo Fisher Scientific. TB Green™ Premix Ex Taq™ II purchased from Takara Biomedical Technology.

2.2 | Preparation of PU and porous nerve film

2.2.1 | Synthesis of PU

PU were successfully fabricated using the in situ polymerization method (Li, Li, et al., 2018). First, 30.00 g of PCL2000 and 7.80 g of IPDI were mixed in a 250 ml three-necked flask under nitrogen atmosphere and heated at 70°C, stirred for 4 hr to obtain the prepolymer. Then, 3.70 g of Lys·OEt-2HCl was applied as a chain extender to extend the prepolymer. After stirring for 2 hr, different contents of gastrodin were added into the mixture to form four different doses of polymers. According to the theoretical weight ratio of gastrodin in polymer chain (set as 0, 0.5, 1, and 5%), the samples were named as PU, 0.5gastrodin/PU, 1gastrodin/PU, and 5gastrodin/PU shown in Table 1, respectively. The resultant mixture was cured at 90°C.

2.2.2 | Preparation of nerve film

Two grams of PU were dissolved in 1, 4-dioxane and 4 g of NaCl particles (<50 μm) as porogen were added into the solution and homogenized for 4 hr, subsequently, poured onto a Teflon mold ($5 \times 5 \times 1$ cm^3). The films were then air-dried for 24 hr, and the salt was leached out from the films by immersion in deionized water under vacuum for 48 hr to form porous films. Finally, the dried film was removed from the Teflon plate to yield PU film with an average thickness of 2 ~3 mm.

2.3 | Characterization

2.3.1 | Morphology observation

The morphology of films was observed by scanning electron microscopy (SEM, FEI Quanta-200, Switzerland) at an accelerating voltage of 10 kV. All samples were mounted onto SEM specimen stubs and sputter-coated with a thin gold for contrast in vacuum.

2.3.2 | Fourier transform infrared spectroscopy (FTIR) and ^{1}H nuclear magnetic resonance (^{1}H NMR) analysis

The functional groups of films were investigated by FTIR (Nicoletis10, Thermo fisher scientific). FTIR spectra of films were collected after averaging 32 scans in the range of 4,000–400 cm^{-1}. The detailed chemical structure was further analyzed by ^{1}H NMR (DRX500, Bruker advance).

2.3.3 | Contact angle

The surface contact angles of films were obtained using a contact angle measurement instrument (JY-82A, Chengde Desheng Testing Instrument, China) at room temperature. A water droplet was deposited on the surface of the film by a microsyringe and photographed. The water contact angle was determined by measuring the angle between film and droplet.

2.3.4 | Thermogravimetric analysis

The thermal stability analysis of the films was tested on a thermogravimetric analysis (TGA/DSC/1600LF, Mettler-Toledo, Switzerland) under nitrogen atmosphere. The temperature ranged from 25 to 600°C at a heating rate of 25°C·min^{-1}.

2.3.5 | Mechanical properties

The tensile mechanical properties of the films were determined using a universal testing machine (Model 3,343, Instron Company).

TABLE 1 The composition of films

Samples	IPDI (g)	PCL2000 (g)	The ratio of NCO:OH in the prepolymer	Lys.OEt-2HCl (g)	Gastrodin content (wt %)
Polyurethane (PU)	7.80	30.00	2.3:1	3.70	–
0.5Gastrodin/PU	7.80	30.00	2.3:1	3.70	0.50
1Gastrodin/PU	7.80	30.00	2.3:1	3.70	1.00
5Gastrodin/PU	7.80	30.00	2.3:1	3.70	5.00

The size of the film was $130 \times 10 \times 2$ cm^3. Samples were pulled until failure at a speed of 200 mm/min to obtain stress–strain curves. The experimental results were performed in quintuplicate for each sample.

2.3.6 | Gel permeation chromatography

The weight-average molecular weights (Mw) and number-average molecular weights (Mn) of the films were conducted with DMF as mobile phase, at room temperature with flow rate of 0.4 ml/min using an instrument (HLC-8320, Tosoh Corporation, Japan). Polymethylmethacrylate was used as the standard.

2.3.7 | Swelling measurements

The swelling ratio of the films was evaluated according to ASTM D570-98 (Asadpour et al., 2018). Dried films (1×1 cm^2) were weighed and submerged in PBS at 37°C. At the pre-determined timepoints of 0.5, 1, 2, 4, 10, 24, 48, and 72 hr, the samples were taken out and removed residual moisture with a filter paper and weighed. Five samples were prepared for each group. The pH values of suspension liquor were measured every week for 4 weeks. The swelling ratio was calculated according to the equation:

$$\text{Swelling ratio}\,(\%) = \frac{Ww - Wd}{Wd} \times 100\%$$

where *Ww* and *Wd* are the weights of the wet and dried specimens, respectively.

2.4 | In vitro cell culture tests

2.4.1 | Cell culture

Biocompatibility investigations on the nerve film with different contents of gastrodin were performed using PC12 cells in vitro. PC12 cells were cultured in 75 cm^2 cell culture flask in DMEM supplemented with 10% FBS, 1% penicillin–streptomycin and incubated at 37°C with 5% CO_2. The culture medium was changed every 3 days.

2.4.2 | Cell viability

After sterilization with γ-ray irradiation with 15 kGy, the films (1×1 cm^2) were seeded with PC12 cells at the density of 2×10^4 cells/well in 24-well plate. The cell viability on films was evaluated using Live/dead reagent following the protocol provided by the manufacturer at day 1 and 3. Live and dead cells were stained green and red, respectively. The specimens were imaged by fluorescence microscopy (EX465-495, Nikon, Japan).

2.4.3 | Cell proliferation and morphology

The cell proliferation on the films for 1, 2, and 3 days was evaluated by CCK-8 assay. At pre-determined timepoints, the culture medium was removed and the cells washed twice by PBS. Approximately 500 μl fresh DMEM containing 50 μl CCK-8 solution was added to each cell sample, and incubated at 37°C for 2.5 hr. Then the supernatant was transferred into 96-well plate with 100 μl/well, the absorbance at 450 nm was measured using Multiskan Spectrum (SpectraMax 190, Molecular Devices Corporation).

Cell morphology on films was studied for 1 and 3 days. The samples were rinsed with PBS, fixed with 2.5% glutaraldehyde for 3 hr, subjected to dehydration with serially diluted alcohol, air-dried, and sputter-coated with gold before examination by SEM.

2.4.4 | Reverse transcription and quantitative polymerase chain reaction

The PC12 cells were seeded in 2×10^4 per well onto films. After incubating 72 hr, the supernatants were collected while cells were used for reverse transcription and quantitative polymerase chain reaction (RT-qPCR) study. The total RNA was isolated using TRIzol reagent and chloroform and isopropanol. In brief, RNA was reverse-transcribed to cDNA using RevertAid First Strand cDNA Synthesis Kit according to the manufacturer's instruction. The resulting cDNA was diluted and used as a template for RT-qPCR in a 20 μl final volume system using TB Green™ Premix Ex Taq™ II. The RT-qPCR was carried out containing the following: 10 μl 2× TB Green Premix Ex Taq II; 1 μl forward primer and 1 μl reverse primer; and 2 μl diluted cDNA. The primers used in the experiments are listed in Table 2. The differences in expression for brain-derived neurotrophic factor (BDNF) and glial cell derived neurotrophic factor (GDNF) between the PU and gastrodin/PU were calculated by normalizing with the β-actin (internal normalized reference), and the target gene expression was presented as relative fold-change based on the value of control sample ($2^{-\triangle\triangle ct}$ method).

2.4.5 | Assay of BDNF concentration in PC12 cells by ELISA

The levels of BDNF in the supernatants of PC12 cells were determined with BDNF ELISA kit (Nanjing Jiancheng Bioengineering Institute, China). The ELISA measurements were performed according to the manufacturer's instructions.

TABLE 2 Primer sequences for RT-qPCR

Gene	Forward primer	Reverse primer
BDNF	TGCGCCCATGAAA GAAGCAAA	CTCAAAAGTGT CAGCCAGGGA
GDNF	CACCAGATAAAC AAGCGGCG	TCGTAGCCCAAA CCCAAGTC
β-Actin	GCTGTGCTATGTT GCCCTAGAC	CCGCTCATTGCCG ATAGTGATG

Abbreviations: BDNF, brain-derived neurotrophic factor; GDNF, glial cell derived neurotrophic factor; RT-qPCR, reverse transcription and quantitative polymerase chain reaction.

2.5 | Statistical analysis

All statistical analyses were performed using the statistical software SPSS 10.0. Data were reported as means ± *SD*. A statistically significant difference was accepted at $p < 0.05$.

3 | RESULTS

3.1 | Physico-chemical properties of the films

3.1.1 | Morphology of the gastrodin/PU films

A PU elastomer incorporated with gastrodin was successfully synthesized in this study (Figure 1a). The SEM images reveal the films to be porous and rough microstructure (Figure 1b,c). The film has pore sizes from 10 to 60 μm throughout the volume of the film, containing mainly interconnected and opened pores. Of note, the microstructure is not obviously changed after adding gastrodin at different contents in the PU matrix.

3.1.2 | Assessment of FTIR and ^{1}H NMR

Chemical structure of gastrodin/PU was characterized by FTIR and ^{1}H NMR (Figure 2). As shown in Figure 2a, the peaks appeared at 2942 cm^{-1} and 2864 cm^{-1} for symmetric and asymmetric vibration of the CH_2 groups of PU, mostly represent the hard and soft segments, respectively (Das, Konwar, Mandal, & Karak, 2013; Lin et al., 2018). The band at 3374 cm^{-1} represents the —NH stretching vibrations in the polymers. A strong peak at 1720 cm^{-1} is ascribed to the carbonyl (C═O) stretching of urethane group (OCONH). The band at 1530 cm^{-1} is associated with —NH in the PU, whereas this peak is not detected in the spectra of PCL and gastrodin. Note that the absorption peak of —$(CH_2)_n$— group at ~732 cm^{-1} arising from PCL segment also appears in PU (Fukushima, Feijoo, & Yang, 2013). Furthermore, the ^{1}H NMR spectra of the 5gastrodin/PU confirms the reaction between gastrodin and IPDI (Figure 2b). The characteristic peaks at 4.05 ppm (f), 2.30 ppm (j), 1.64 ppm (g, i) and 1.37 ppm (h) of PCL (Cassan et al., 2018), 0.9–1.0 ppm (d, e) of IPDI (Makal, Uslu, & Wynne, 2007), can be clearly identified. The protons close to the urethane functional groups are also observed at range of 3.86–-3.88 ppm (Javaid et al., 2018) (b). In addition, the peak at 7.01 ppm (a, c) is attributed to the gastrodin (Baek et al., 1999), which is absent in the PU (Figure S1).

3.1.3 | Mechanical properties of the films

Figure 3 shows the tensile mechanical properties of our films. A sorely stiff matrix inhibits the growth and function of nerve cells. The elasticity and excellent resistance to distortion (Figure 3a) may be an appropriate feature to integration with native tissue (Asadpour et al., 2018). After functionalized with gastrodin, the modulus of the gastrodin/PU films are all improved, also evidenced by the shape of tensile stress–strain curves (Figure 3d). The Young' modulus of 5gastrodin/PU (3.38 ± 0.02 MPa), 1gastrodin/PU (1.75 ± 0.09 MPa), and 0.5gastrodin/PU (1.56 ± 0.22 MPa) are significantly higher than that of the PU group (0.83 ± 0.05 MPa; Figure 3c). However, the film elongation at break is greatly reduced after gastrodin addition. Interestingly, the elongation at break for all gastrodin/PU films has not detectable significance (Figure 3b).

The thermal stability of synthesized polymer was analyzed by TGA and the curves were plotted in Figure 3e. It shows that the weight gradually decreases as the temperature increases. Peak at about 350°C represents main weight loss, which indicates break down of chemical bonds between hard and soft segments. The thermal stability presents uptrend with addition of gastrodin. Furthermore, in Table 3, the number-average molecular weight (Mn) of 5gastrodin/PU (12,134 g/mol) is higher than PU (9473 g/mol) according to GPC measurement. The relative lower polydispersity index (PDI) of 5gastrodin/PU indicates more concentrated molecular weight distribution.

3.1.4 | Contact angle and swelling rate

Water contact angle was carried out to determine the surface hydrophilicity of the films (Figure 4a). The surface wettability results show that the 5gastrodin/PU has the lowest contact angle (32.90°, $p < 0.001$), indicating highly hydrophilic feature of this polymer as expected, while the pure PU has the highest contact angle (93.17°, $p < 0.05$) and hydrophobicity among the groups. As shown in Figure 4b, the swelling ratio of the gastrodin/PU increases from 146 to 219% with the weight ratio of gastrodin to PU increasing from 0 to 5%.

The change of pH values is also presented in Figure 4c. The pH values drop dramatically after 1 week and slightly increase to 6.7 with time. Obviously, 5gastrodin/PU is closer to neutral throughout the degradation process, which provides a proper microenvironment for cell growth and tissue regeneration.

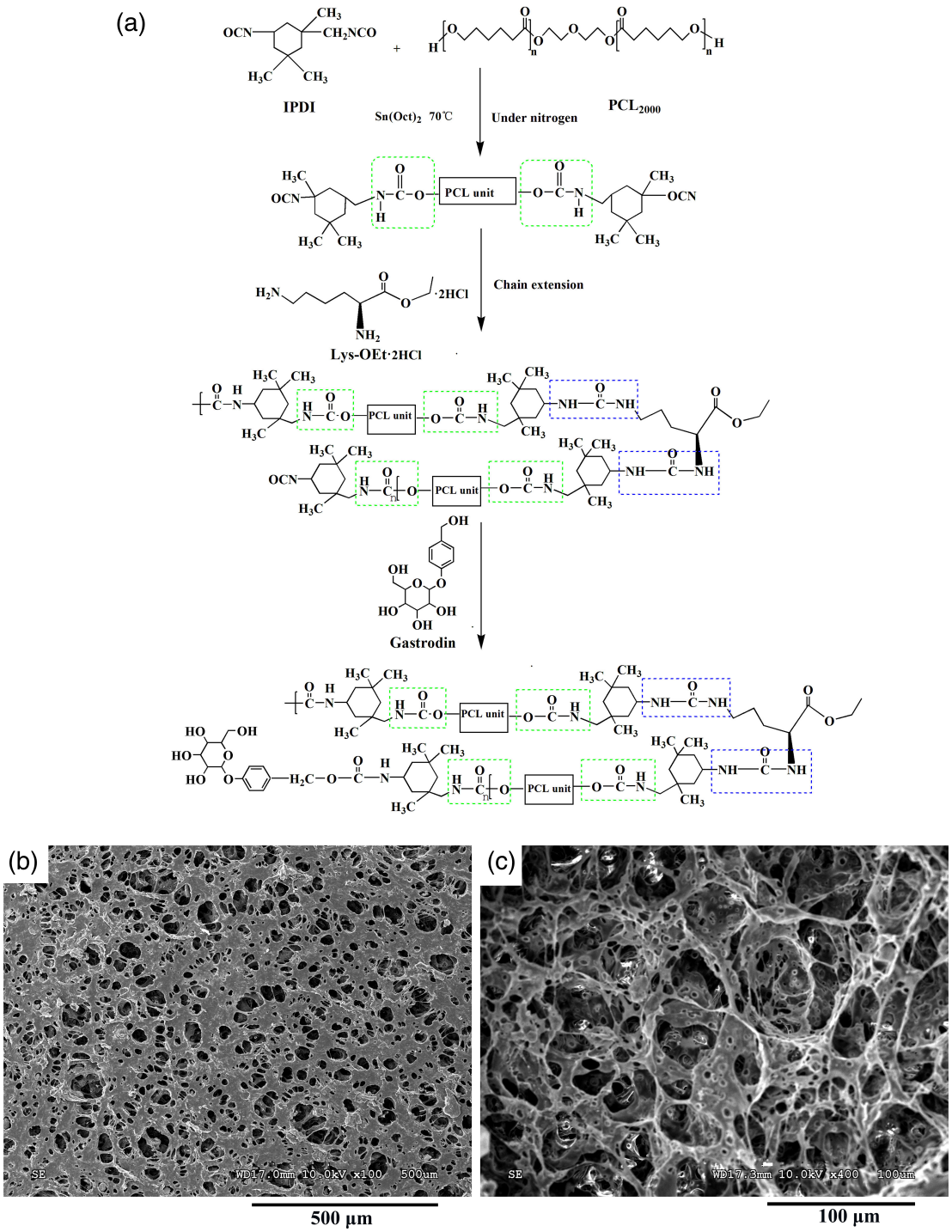

FIGURE 1 The chemical structure and the porous structure of the PU films. (a) The synthetic process. (b, c) SEM images of PU with controlled microstructure magnified by (b) ×100 and (c) ×400. PU, polyurethane; SEM, scanning electron microscopy

3.2 | Biocompatibility of the films

3.2.1 | Cell morphology and viability

Non-cytotoxicity is generally considered to be essential for tissue engineering materials. The gastrodin/PU is available for cell survival showing neither gastrodin nor PU is cytotoxic. We evaluated the effect of films on morphology and activity of neuron-like PC12 cells. The live/dead assay performed for PC12 seeded onto films after day 1 and day 3 further shows little dead cells (Figure 5). After 1-day culture time, the PC12 cells become rapidly confluent on the gastrodin/PU films and majority express a bipolar configuration while on the PU film retain cobblestone morphology (Figure 5a–d). On day 3, a well spread and bridging the pores morphology of live PC12 cells (green,

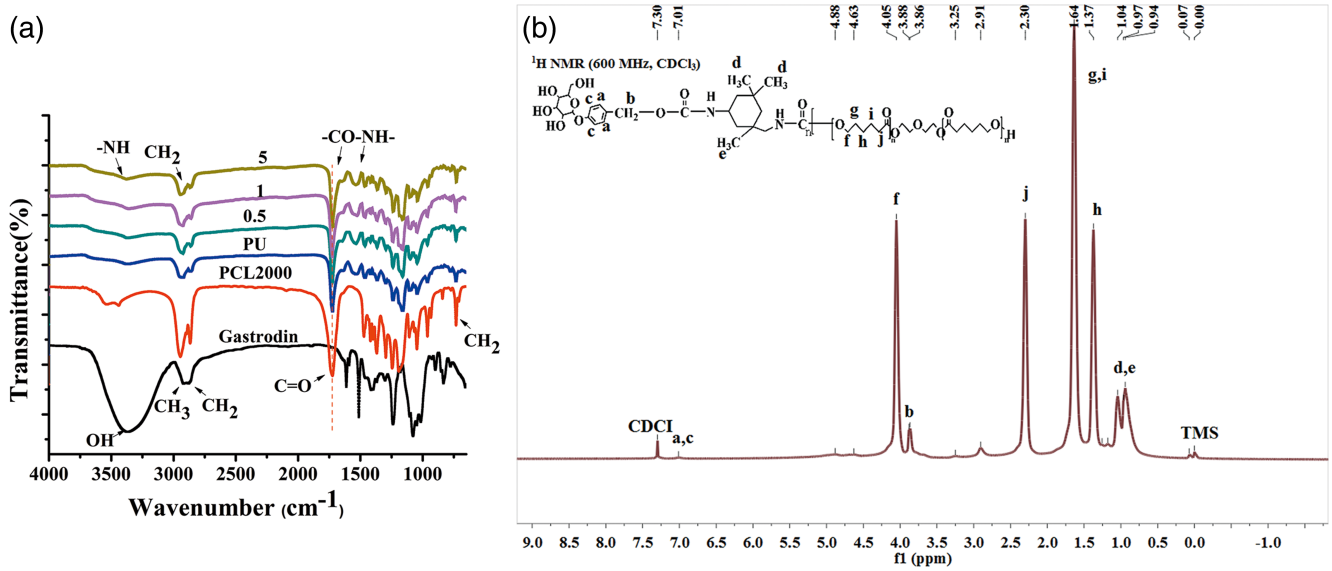

FIGURE 2 (a) FTIR spectra of gastrodin, PCL2000, and PUs. (b) ^{1}H NMR spectrum of 5Gastrodin/PU. FTIR, Fourier transform infrared spectroscopy; ^{1}H NMR, ^{1}H nuclear magnetic resonance; PU, polyurethane

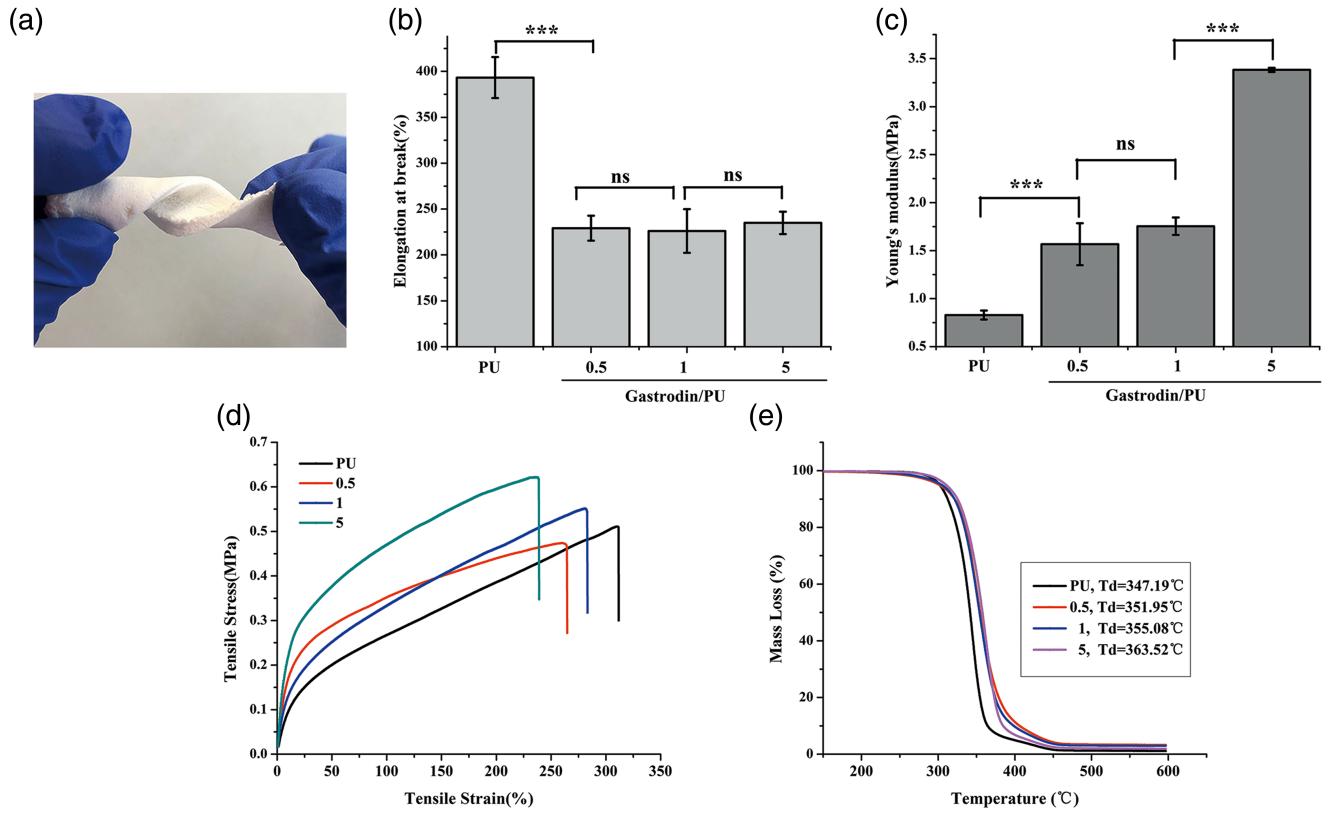

FIGURE 3 (a) Macrograph of resistance to distortion. Effects of Gastrodin content on the (b) elongation at break, (c) Young' modulus, (d) tensile stress–strain curves, and (e) thermogravimetric (TG) curves of films. ***p < 0.001; ns: no significant difference

Figure 5f–h) compared with a few dead cells (red, Figure 5e) in PU film are seen. This is especially evident in the 5gastrodin/PU film that presents long neurite extensions that are typical of mature and functional neurons.

In Figure 6, SEM images reveal that most of the area of the surface of films is covered with the cells. PC12 cells are well adhered on gastrodin/PU films and exhibit a typical fusiform morphology (Figure 6b–d), while the cells on the PU film are

poorly attached (Figure 6a) for 1 day. When cultured for 3 days, the cells show better cell growth with the long neurite extension and seem to exhibit a better interconnected neural network on gastrodin/PU films than PU film. The proliferated cells have occupied most surfaces, and the cells tend to elongate progressively with time; and typical bipolar processes can be observed after 3 days of culture in gastrodin/PU. Moreover, the cells spread with numerous neurites and grow into the pores, presenting more complete morphology on the gastrodin/PU films (Figure 6f–h). The prominent neurite extensions support the results from live/dead images. However, the cells on the PU film express a rounded morphology with very few, if any, neurites (Figure 6e). This difference in the response of the films is also reflected in the cell proliferation from CCK-8 results (Figure 6i). While all groups exhibit significant increase in the cell proliferation with time, and gastrodin accelerates cell proliferate at predetermined time point, the proliferation of 5gastrodin/PU group is found to progressively increased unlike their counterparts which show moderate growth, suggesting that gastrodin may promote a positive environment that facilitates cell survival. The combined results demonstrate that the PU films functionalized with gastrodin have good cytocompatibility.

TABLE 3 Comparison of the molecular weight parameters of polyurethanes (PUs)

Samples	Mn (g/mol)	Mw (g/mol)	Mw/Mn (PDI)
PU	9473	828,815	87.494
5Gastrodin/PU	12,134	264,657	21.810

3.2.2 | Gene expressions

The relative quantitative gene expression level induced by the films was investigated. As shown in Figure 6k,l, 5gastrodin/PU group

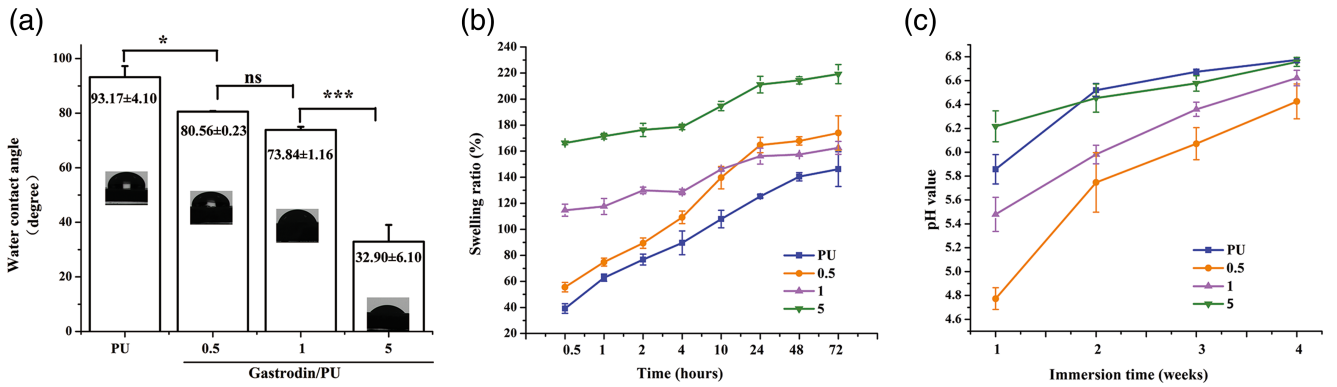

FIGURE 4 (a) Surface wettability of films. (b) The swelling ratio of specimens. (c) The pH values of the films, which were immersed in PBS and incubated at 37°C for 4 weeks. ***$p < 0.001$; **$p < 0.001$; *$p < 0.05$; ns: no significant difference

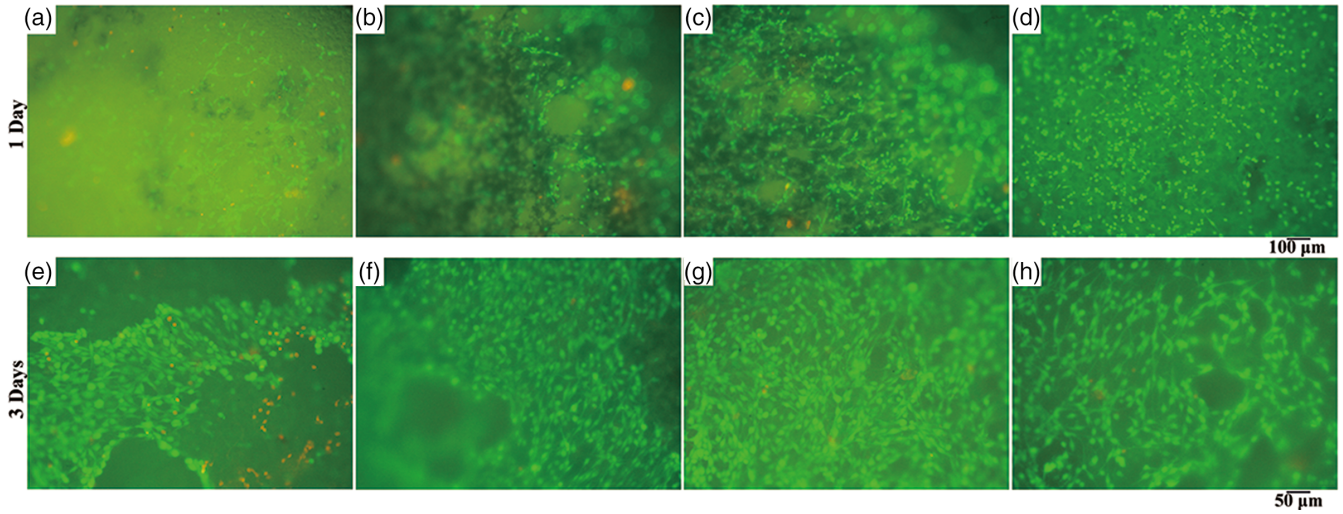

FIGURE 5 Cytocompatibility of films for PC12 cells. Live/dead staining of PC12 cells on the films cultured for 1 and 3 days. (a, e) PU. (b, f) 0.5Gastrodin/PU. (c, g) 1Gastrodin/PU. (d,h) 5Gastrodin/PU. Live cells are stained green, dead cells are stained red. PU, polyurethane

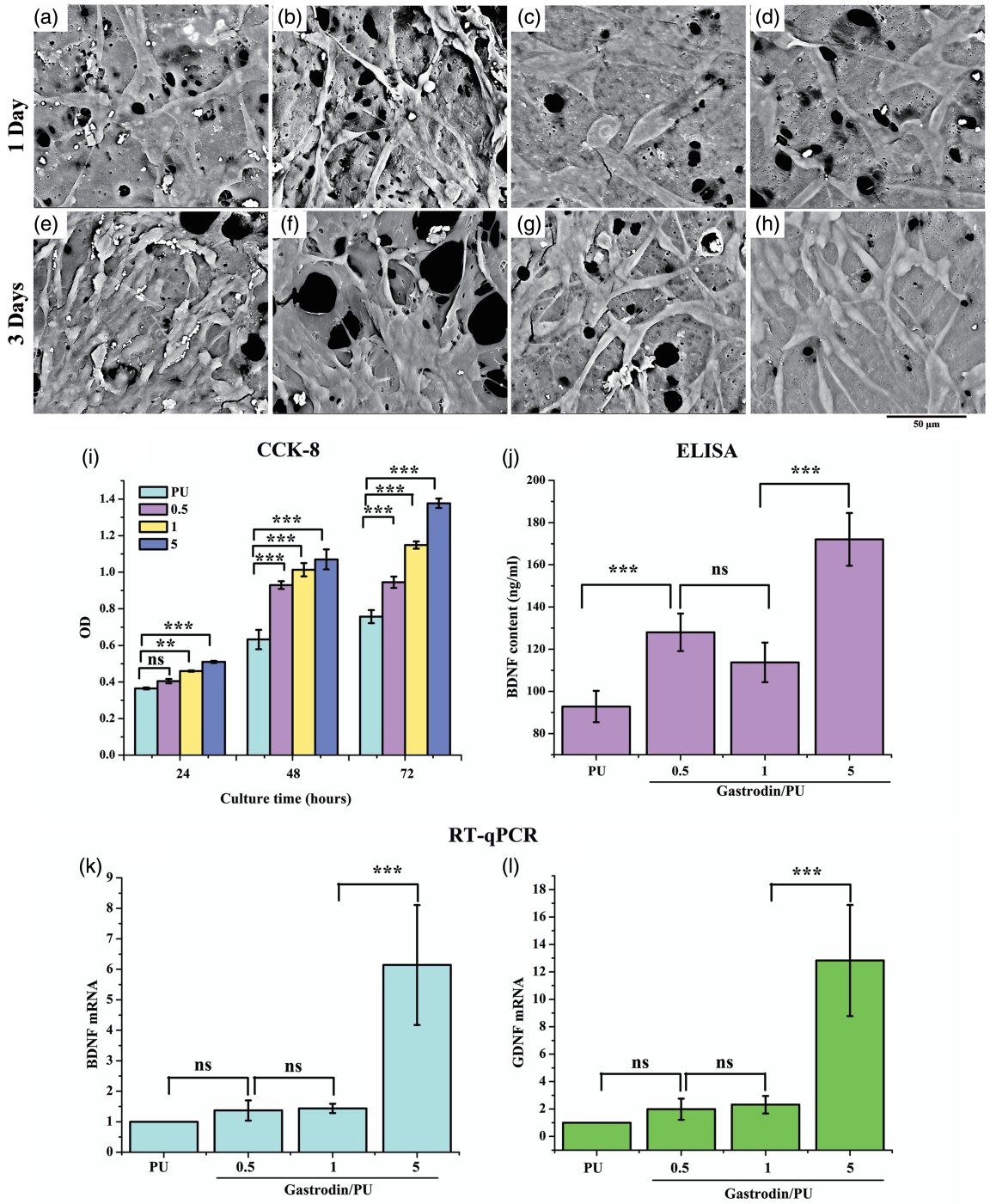

FIGURE 6 The morphology of PC12 cells cultured on films after 1 and 3 days, and the effects of Gastrodin content in the PU matrix on factors expression after 3 days of cell seeding. (a,e) PU. (b,f) 0.5Gastrodin/PU. (c,g) 1Gastrodin/PU. (d,h) 5Gastrodin/PU. The results indicate that the films are biocompatible, the cell adhesion and spread on the surface of the Gastrodin/PU films are superior as compared with the PU. (i) Viability of PC12 cell using CCK-8 kit. ***$p < 0.001$; **$p < 0.001$; ns: no significant difference. (j) Elisa analysis of BDNF. RT-qPCR for BDNF (k) and GDNF factors (l). BDNF, brain-derived neurotrophic factor; GDNF, glial cell derived neurotrophic factor; PU, PU, polyurethane

exhibits a significantly higher gene expression of BDNF (6.14 ± 1.96-fold) and GDNF (12.82 ± 4.0-fold) in comparison with the other groups ($p < 0.001$). Moreover, the protein expression level for BDNF also increases as the gastrodin content increased (Figure 6j). The results further suggest that the 5gastrodin/PU can significantly promote the secretion of neurotrophic factors and is a suitable biomaterial for PC12 cell adhesion, growth, proliferation, and neurogenic differentiation.

4 | DISCUSSION

The development of engineered nerve guide conduits is progressively emerging as a powerful strategy in the field of peripheral nerve surgery. Nerve guide conduits provide opportunities to control the microenvironment for enhanced nerve regeneration (Oh et al., 2018). A biomaterial with biomimetic properties (pore structures, surface, and chemical/mechanical properties) allows better cell function and adequate exchange of oxygen and nutrients, while providing the necessary barrier to prevent the infiltration of unwanted tissues into the scaffold from outside and exiting of cells and growth factors from inside to outside of the channel (Ezra, Bushman, Shreiber, Schachner, & Kohn, 2016; Kim et al., 2018). To improve mechanical qualities and nerve differentiation, we have considered the microstructure design of our gastrodin/PU film, including the gastrodin modification of PU soft segment, and the formation of porous structure. At a microlevel, a porous structure has a pore size of approximately 10~60 μm (Figure 1), which has been demonstrated to help Schwann cell migration from proximal end to distal end of the nerve injury and promoted axon penetration (Manoukian et al., 2019; Singh, Shiekh, Das, Seppälä, & Kumar, 2018); and high interconnective porous structure is desirable for neural tissue engineering as it can facilitate better diffusion of oxygen and nutrients as well as enable cell infiltration and penetration to establish three dimensional network (Figure 6), further promotes peripheral nerve regeneration (Hsu & Ni, 2008; Oh et al., 2008). At a nano-level, the hard/soft nanodomain structure of PU matrix in our previous study (Li et al., 2015) may provide a positive environmental stimulus for nerve fiber regrowth. This unique microstructure can be believed to be similar to the segmented collagen, and porous structure of natural nerve, which is vitally important to high-performance film that is employed for nerve regeneration and functional recovery.

The properties of matrix and the molecular interaction of chain segment have a strong impact on mechanical quality of films. In comparison with pure PU, the increased hydroxyl value of gastrodin can promote its polymerization reaction and tight intermolecular forces in gastrodin/PU. Block PU is structured with hard/soft segments, its motion behavior mainly depends on the segment structure, molecular weight, and the interaction between the hard and soft segments. The higher Mn and lower PDI of 5gastrodin/PU matrix lead to an increase in strength (Table 3). In addition, native aromatic macromolecular structure and increasing cross-linking density endowed by the polyols of gastrodin also contribute to the strength. The elongation at break presents an opposite trend, probably because a large amount of unreacted dangling groups existing in PU matrix weaken the matrix resistance to external tension. The improved modulus as gastrodin content is consistent with the enhanced thermal stability. The gastrodin with higher hydroxyl number gives PU matrix more types of polar-polar interactions with urethane, and hydrogen bonding within its molecular chains. Similar results were also reflected in our previous report (Li, Li, et al., 2018). The appropriate mechanical properties endow the nerve biomaterials to resist mechanical forces and environmental pressures without collapsing during in vitro and in vivo conditions (Chiono & Tonda-Turo, 2015). Additionally, nerve biomaterials need to be flexible enough as high rigidity could damage regenerated axons and surrounding tissues (Yucel, Kose, & Hasirci, 2010).

The surface property of the biomaterial in terms of hydrophilicity is another key factor that influences its biological efficiency (Chang & Wang, 2011). Similar to soft tissues, a highly hydrated biomaterial can facilitate the early stage of cell adhesion onto the biomaterial surface (Asadpour et al., 2018). The wettability of 5gastrodin/PU is remarkedly increased (Figure 4a). The presence of gastrodin in the PU matrix endows the gastrodin/PU with hydrophilic character, which has the ability to form hydrogen-bonding interaction with water molecules. The swelling behavior as determined by water absorption rate is also related to matrix hydrophilicity, which presents similar trends as wettability (Figure 4b). The hydrophilic nature of gastrodin is favorable for water absorption. The water absorption capacity of the gastrodin/PU increases, probably because gastrodin incorporated into film promotes the contact between the polymeric substrate and water. Swelling properties of the biomaterials affect degradation rate, the nutrition diffusion, and waste transfer rate within the biomaterials (Asadpour et al., 2018). Additionally, the hydrophilic substrate is beneficial to cell attachment and proliferation; hence, the gastrodin incorporated is expected to improve the biocompatibility of the gastrodin/PU films (Figure 5).

The cell culture results, including cell viability and CCK-8 (Figure 6i) demonstrate that the gastrodin/PU porous films, especially 5gastrodin/PU, can promote cell attachment, spread and proliferation. In addition to superior activity, the nerve differentiation capacity of gastrodin plays a crucial role in nerve regeneration. The SEM images exhibit positive influence on neurite growth for 5gastrodin/PU (Figure 6d,h). Neurotrophic factors (NTFs) analysis further reveals upregulated expression levels. A synergistic effect of elevated BDNF and GDNF can accelerate the regrowth of regenerating axons and allow better functional recovery (Santos, Giudetti, Micera, Navarro, & del Valle, 1636). A possible explanation for this would be improved hydrophilicity and supported cells adherence and trigger neurite outgrowth. When the cells attach to the biomaterial surface, a sequence of physical and chemical interactions happen between them leading to modulation of extracellular matrix deposition as well as cell proliferation and differentiation (Wang et al., 2017). The initial cell adhesive response to the surface of biomaterials is important for the biocompatibility. The hydrophilic characteristics of functionalized with gastrodin provide a more suitable environment conducive for improved cell adhesion and proliferation on 5gastrodin/PU film.

5 | CONCLUSION

We designed and fabricated a porous system based on gastrodin and elastomer PU, for potential use in nerve regeneration. The gastrodin/PU porous film has desirable flexibility and supporting mechanical strength. The enhanced molecular interaction between polyfunctional gastrodin and PU matrix is a dominating factor in the mechanical

improvement of gastrodin/PU. The pore size (10~60 μm) and interconnectivity are efficient for cell growth and tissue infiltration. The gastrodin in the PU matrix improves hydrophilicity, and further promotes cell activity. The 5gastrodin/PU film not only supports PC12 cell attachment, but also maintains cells with more neurite extension concomitantly with up-regulation of BDNF and GDNF expression levels. Thus, the 5gastrodin/PU film may be potentially constructed as a suitable conduit with a porous 3D microstructure and excellent biocompatibility for neural tissue engineering.

ACKNOWLEDGMENTS

This research was supported by National Natural Science Foundation of China (81360200/81460210/81860326), the Department of Science and Technology of Yunnan Province of China (2017FA035/2018FE001(-137)/2018FE001(-165)/2019ZF011-2), International Science and Technology Cooperation Project of Yunnan Province (2018IA048), and Education Commission of Yunnan Province (2017zzx200/2018Y046), Program for Innovative Research Team (in Science and Technology) in University of Yunnan Province.

CONFLICTS OF INTEREST

The authors declare no competing financial interest.

REFERENCES

Arévalo, F., Uscategui, Y. L., Diaz, L., Cobo, M., & Valero, M. F. (2016). Effect of the incorporation of chitosan on the physico-chemical, mechanical properties and biological activity on a mixture of polycaprolactone and polyurethanes obtained from castor oil. *Journal of Biomaterials Applications*, *31*(5), 708–720.

Asadpour, S., Yeganeh, H., Ai, J., Kargozar, S., Rashtbar, M., Seifalian, A., & Ghanbari, H. (2018). Polyurethane-polycaprolactone blend patches: Scaffold characterization and cardiomyoblast adhesion, proliferation, and function. *ACS Biomaterials Science & Engineering*, *4*(12), 4299–4310.

Baek, N. I., Choi, S. Y., Park, J. K., Cho, S. W., Ahn, E. M., Jeon, S. G., … Shon, I. H. (1999). Isolation and identification of succinic semialdehyde dehydrogenase inhibitory compound from the rhizome ofGastrodia elata blume. *Archives of Pharmacal Research*, *22*(2), 219–224.

Cassan, D., Sydow, S., Schmidt, N., Behrens, P., Roger, Y., Hoffmann, A., … Menzel, H. (2018). Attachment of nanoparticulate drug-release systems on poly(ε-caprolactone) nanofibers via a graftpolymer as interlayer. *Colloids and Surfaces B: Biointerfaces*, *163*, 309–320.

Cattin, A. L., Burden Jemima, J., Van Emmenis, L., Mackenzie Francesca, E., Hoving Julian, J. A., Garcia Calavia, N., … Lloyd, A. C. (2015). Macrophage-induced blood vessels guide schwann cell-mediated regeneration of peripheral nerves. *Cell*, *162*(5), 1127–1139.

Chang, H. I., & Wang, Y. (2011). Cell responses to surface and architecture of tissue engineering scaffolds. *Regenerative Medicine and Tissue Engineering––Cells and Biomaterials*, *21983*.

Chang, Y. C., Chen, M. H., Liao, S. Y., Wu, H. C., Kuan, C. H., Sun, J. S., & Wang, T. W. (2017). Multichanneled nerve guidance conduit with spatial gradients of neurotrophic factors and oriented nanotopography for repairing the peripheral nervous system. *ACS Applied Materials & Interfaces*, *9*(43), 37623–37636.

Chen, W., di Carlo, C., Devery, D., McGrath, D. J., McHugh, P. E., Kleinsteinberg, K., … Kok, R. J. (2018). Fabrication and characterization of gefitinib-releasing polyurethane foam as a coating for drug-eluting stent in the treatment of bronchotracheal cancer. *International Journal of Pharmaceutics*, *548*(2), 803–811.

Chiono, V., & Tonda-Turo, C. (2015). Trends in the design of nerve guidance channels in peripheral nerve tissue engineering. *Progress in Neurobiology*, *131*, 87–104.

Dai, J. N., Zong, Y., Zhong, L. M., Li, Y. M., Zhang, W., Bian, L. G., … Lu, D. (2011). Gastrodin inhibits expression of inducible NO synthase, cyclooxygenase-2 and proinflammatory cytokines in cultured LPS-stimulated microglia via MAPK pathways. *PLoS One*, *6*(7), e21891.

Das, B., Konwar, U., Mandal, M., & Karak, N. (2013). Sunflower oil based biodegradable hyperbranched polyurethane as a thin film material. *Industrial Crops and Products*, *44*, 396–404.

Dezhznz, Y., Xiao Hong, W., Yongnian, Y., & Renji, Z. (2007). Preliminary studies on peripheral nerve regeneration using a new polyurethane conduit. *Journal of Bioactive and Compatible Polymers*, *22*(2), 143–159.

Dixon, A. R., Jariwala, S. H., Bilis, Z., Loverde, J. R., Pasquina, P. F., & Alvarez, L. M. (2018). Bridging the gap in peripheral nerve repair with 3D printed and bioprinted conduits. *Biomaterials*, *186*, 44–63.

Ezra, M., Bushman, J., Shreiber, D., Schachner, M., & Kohn, J. (2016). Porous and nonporous nerve conduits: The effects of a hydrogel luminal filler with and without a neurite-promoting moiety. *Tissue Engineering Part A*, *22*(9–10), 818–826.

Farzamfar, S., Ehterami, A., Salehi, M., Vaeez, A., Atashi, A., & Sahrapeyma, H. (2019). Unrestricted somatic stem cells loaded in nanofibrous conduit as potential candidate for sciatic nerve regeneration. *Journal of Molecular Neuroscience*, *67*(1), 48–61.

Fukushima, K., Feijoo, J. L., & Yang, M. C. (2013). Comparison of abiotic and biotic degradation of PDLLA, PCL and partially miscible PDLLA/PCL blend. *European Polymer Journal*, *49*(3), 706–717.

Grzesiak, J., Lis, A., Szarek, D., Laska, J., Marycz, K., & Fryczkowski, R. (2015). Characterization of olfactory ensheathing glial cells cultured on polyurethane/polylactide electrospun nonwovens. *International Journal of Polymer Science*, *2015*, 908328.

Gu, X., Ding, F., Yang, Y., & Liu, J. (2011). Construction of tissue engineered nerve grafts and their application in peripheral nerve regeneration. *Progress in Neurobiology*, *93*(2), 204–230.

Hahm, J.-I. (2014). Fundamentals of nanoscale polymer–protein interactions and potential contributions to solid-state nanobioarrays. *Langmuir*, *30*(33), 9891–9904.

Hsu, S. H., & Ni, H. C. (2008). Fabrication of the microgrooved/microporous polylactide substrates as peripheral nerve conduits and in vivo evaluation. *Tissue Engineering Part A*, *15*(6), 1381–1390.

Javaid, M. A., Khera, R. A., Zia, K. M., Saito, K., Bhatti, I. A., & Asghar, M. (2018). Synthesis and characterization of chitosan modified polyurethane bio-nanocomposites with biomedical potential. *International Journal of Biological Macromolecules*, *115*, 375–384.

Jeon, T., Vutescu, E. S., Saltzman, E. B., Villa, J. C., Wolfe, S. W., Lee, S. K., … Sneag, D. B. (2018). Evaluation of two collagen conduits and autograft in rabbit sciatic nerve regeneration with quantitative magnetic resonance DTI, electrophysiology, and histology. *European Radiology Experimental*, *2*(1), 19.

Kehoe, S., Zhang, X. F., & Boyd, D. (2012). FDA approved guidance conduits and wraps for peripheral nerve injury: A review of materials and efficacy. *Injury*, *43*(5), 553–572.

Kim, S. M., Lee, M. S., Jeon, J., Lee, D. H., Yang, K., Cho, S. W., … Yang, H. S. (2018). Biodegradable nerve guidance conduit with microporous and micropatterned poly(lactic-co-glycolic acid)-accelerated sciatic nerve regeneration. *Macromolecular Bioscience*, *18*(12), 1800290.

Labroo, P., Hilgart, D., Davis, B., Lambert, C., Sant, H., Gale, B., … Agarwal, J. (2019). Drug-delivering nerve conduit improves regeneration in a critical-sized gap. *Biotechnology and Bioengineering*, *116*(1), 143–154.

Li, G., Xue, C., Wang, H., Yang, X., Zhao, Y., Zhang, L., & Yang, Y. (2018). Spatially featured porous chitosan conduits with micropatterned inner

wall and seamless sidewall for bridging peripheral nerve regeneration. *Carbohydrate Polymers*, *194*, 225–235.

Li, L., Li, Q., Yang, J., Sun, L., Guo, J., Yao, Y., … Lu, D. (2018). Enhancement in mechanical properties and cell activity of polyurethane scaffold derived from gastrodin. *Materials Letters*, *228*, 435–438.

Li, L., Zuo, Y., Zou, Q., Yang, B., Lin, L., Li, J., & Li, Y. (2015). Hierarchical structure and mechanical improvement of an n-HA/GCO-PU composite scaffold for bone regeneration. *ACS Applied Materials & Interfaces*, *7* (40), 22618–22629.

Lin, L., Ma, J., Mei, Q., Cai, B., Chen, J., Zuo, Y., … Li, Y. (2018). Elastomeric polyurethane foams incorporated with nanosized hydroxyapatite fillers for plastic reconstruction. *Nanomaterials*, *8*(12), 972.

Makal, U., Uslu, N., & Wynne, K. J. (2007). Water makes it hydrophobic: Contraphilic wetting for polyurethanes with soft blocks having semi-fluorinated and 5,5-Dimethylhydantoin side chains. *Langmuir*, *23*(1), 209–216.

Manoukian, O. S., Arul, M. R., Rudraiah, S., Kalajzic, I., & Kumbar, S. G. (2019). Aligned microchannel polymer-nanotube composites for peripheral nerve regeneration: Small molecule drug delivery. *Journal of Controlled Release*, *296*, 54–67.

Mokarram, N., Merchant, A., Mukhatyar, V., Patel, G., & Bellamkonda, R. V. (2012). Effect of modulating macrophage phenotype on peripheral nerve repair. *Biomaterials*, *33*(34), 8793–8801.

Niu, Y., Chen, K. C., He, T., Yu, W., Huang, S., & Xu, K. (2014). Scaffolds from block polyurethanes based on poly(ε-caprolactone) (PCL) and poly(ethylene glycol) (PEG) for peripheral nerve regeneration. *Biomaterials*, *35*(14), 4266–4277.

Niu, Y., Li, L., Chen, K. C., Chen, F., Liu, X., Ye, J., … Xu, K. (2015). Scaffolds from alternating block polyurethanes of poly(ε-caprolactone) and poly(ethylene glycol) with stimulation and guidance of nerve growth and better nerve repair than autograft. *Journal of Biomedical Materials Research Part A*, *103*(7), 2355–2364.

Nune, M., Krishnan, U. M., & Sethuraman, S. (2016). PLGA nanofibers blended with designer self-assembling peptides for peripheral neural regeneration. *Materials Science and Engineering: C*, *62*, 329–337.

Oh, S. H., Kang, J. G., Kim, T. H., Namgung, U., Song, K. S., Jeon, B. H., & Lee, J. H. (2018). Enhanced peripheral nerve regeneration through asymmetrically porous nerve guide conduit with nerve growth factor gradient. *Journal of Biomedical Materials Research Part A*, *106*(1), 52–64.

Oh, S. H., Kim, J. H., Song, K. S., Jeon, B. H., Yoon, J. H., Seo, T. B., … Lee, J. H. (2008). Peripheral nerve regeneration within an asymmetrically porous PLGA/Pluronic F127 nerve guide conduit. *Biomaterials*, *29*(11), 1601–1609.

Palumbo, C., Massa, R., Panico, M., Di Muzio, A., Sinibaldi, P., Bernardi, G., & Modesti, A. (2002). Peripheral nerve extracellular matrix remodeling in Charcot-Marie-Tooth type I disease. *Acta Neuropathologica*, *104*(3), 287–296.

Peng, Z., Wang, S., Chen, G., Cai, M., Liu, R., Deng, J., … Hai, C. (2015). Gastrodin alleviates cerebral ischemic damage in mice by improving anti-oxidant and anti-inflammation activities and inhibiting apoptosis pathway. *Neurochemical Research*, *40*(4), 661–673.

Princi, E., Vicini, S., Stagnaro, P., & Conzatti, L. (2011). The nanostructured morphology of linear polyurethanes observed by transmission electron microscopy. *Micron*, *42*(1), 3–7.

Saeki, M., Tanaka, K., Imatani, J., Okamoto, H., Watanabe, K., Nakamura, T., … Hirata, H. (2018). Efficacy and safety of novel collagen conduits filled with collagen filaments to treat patients with peripheral nerve injury: A multicenter, controlled, open-label clinical trial. *Injury*, *49*(4), 766–774.

Salehi, M., Naseri-Nosar, M., Ebrahimi-Barough, S., Nourani, M., Khojasteh, A., Farzamfar, S., … Ai, J. (2018). Polyurethane/Gelatin nanofibrils neural guidance conduit containing platelet-rich plasma and melatonin for transplantation of Schwann cells. *Cellular and Molecular Neurobiology*, *38*(3), 703–713.

Santos, D., Giudetti, G., Micera, S., Navarro, X., & del Valle, J. (1636). Focal release of neurotrophic factors by biodegradable microspheres enhance motor and sensory axonal regeneration in vitro and in vivo. *Brain Research*, *2016*, 93–106.

Shahriari, D., Koffler, J. Y., Tuszynski, M. H., Campana, W. M., & Sakamoto, J. S. (2017). Hierarchically ordered porous and high-volume polycaprolactone microchannel scaffolds enhanced axon growth in transected spinal cords. *Tissue Engineering Part A*, *23*(9–10), 415–425.

Shahriari, D., Shibayama, M., Lynam, D. A., Wolf, K. J., Kubota, G., Koffler, J. Y., … Sakamoto, J. S. (2017). Peripheral nerve growth within a hydrogel microchannel scaffold supported by a kink-resistant conduit. *Journal of Biomedical Materials Research Part A*, *105*(12), 3392–3399.

Shoaib, M., Ur Rahman, M. S., Saeed, A., & Naseer, M. M. (2018). Mesoporous bioactive glass-polyurethane nanocomposites as reservoirs for sustained drug delivery. *Colloids and Surfaces B: Biointerfaces*, *172*, 806–811.

Singh, A., Shiekh, P., Das, M. V., Seppälä, J., & Kumar, A. (2018). Aligned chitosan-gelatin cryogel filled polyurethane nerve guidance channel for neural tissue engineering: Fabrication, characterization and in-vitro evaluation. *Biomacromolecules*, *20*(2), 662–673.

Sridharan, R., Reilly, R. B., & Buckley, C. T. (2015). Decellularized grafts with axially aligned channels for peripheral nerve regeneration. *Journal of the Mechanical Behavior of Biomedical Materials*, *41*, 124–135.

Uscátegui, L. Y., Díaz, E. L., Gómez-Tejedor, A. J., Vallés-Lluch, A., Vilariño-Feltrer, G., Serrano, A. M., & Valero, F. M. (2019). Candidate polyurethanes based on castor oil (*Ricinus communis*), with polycaprolactone diol and chitosan additions, for use in biomedical applications. *Molecules*, *24*(2), 237.

Vijayavenkataraman, S., Thaharah, S., Zhang, S., Lu, W. F., & Fuh, J. Y. H. (2018). 3D-Printed PCL/rGO conductive scaffolds for peripheral nerve injury repair. *Artificial Organs*, *43*(5), 515–523.

Vikström, P., Björkman, A., Carlsson, I. K., Olsson, A.-K., & Rosén, B. (2018). Atypical sensory processing pattern following median or ulnar nerve injury—A case-control study. *BMC Neurology*, *18*(1), 146.

Wang, H., Zhang, R., Qiao, Y., Xue, F., Nie, H., Zhang, Z., … Tan, Q. (2014). Gastrodin ameliorates depression-like behaviors and up-regulates proliferation of hippocampal-derived neural stem cells in rats: Involvement of its anti-inflammatory action. *Behavioural Brain Research*, *266*, 153–160.

Wang, S., Sun, C., Guan, S., Li, W., Xu, J., Ge, D., … Ma, X. (2017). Chitosan/gelatin porous scaffolds assembled with conductive poly(3,-4-ethylenedioxythiophene) nanoparticles for neural tissue engineering. *Journal of Materials Chemistry B*, *5*(24), 4774–4788.

Wang, X. L., Xing, G. H., Hong, B., Li, X. M., Zou, Y., Zhang, X. J., & Dong, M. X. (2014). Gastrodin prevents motor deficits and oxidative stress in the MPTP mouse model of Parkinson's disease: Involvement of ERK1/2–Nrf2 signaling pathway. *Life Sciences*, *114*(2), 77–85.

Wang, Y., Peng, J., Zhao, Z., Huang, J., Zhao, B., Zhang, L., … Lu, S. (2010). Extraction techniques and biocompatibility evaluations of naturally derived nerve extracellular matrix. *Zhongguo Xiu Fu Chong Jian Wai Ke Za Zhi*, *24*(9), 1128–1132.

Wu, H., Fang, Q., Liu, J., Yu, X., Xu, Y., Wan, Y., & Xiao, B. (2018). Multi-tubule conduit-filler constructs loaded with gradient-distributed growth factors for neural tissue engineering applications. *Journal of the Mechanical Behavior of Biomedical Materials*, *77*, 671–682.

Xu, X. (2007). Protective effects of gastrodin on hypoxia-induced toxicity in primary cultures of rat cortical neurons. *Planta Medica*, *73*(7), 650–654.

Yucel, D., Kose, G. T., & Hasirci, V. (2010). Polyester based nerve guidance conduit design. *Biomaterials*, *31*(7), 1596–1603.

Zhang, W., Wray, L. S., Rnjak-Kovacina, J., Xu, L., Zou, D., Wang, S., … Jiang, X. (2015). Vascularization of hollow channel-modified porous silk scaffolds with endothelial cells for tissue regeneration. *Biomaterials*, *56*, 68–77.

Zou, J. L., Liu, S., Sun, J. H., Yang, W. H., Xu, Y. W., Rao, Z. L., … Zeng, Y.-S. (2018). Peripheral nerve-derived matrix hydrogel promotes

remyelination and inhibits synapse formation. *Advanced Functional Materials*, *28*(13), 1705739.

SUPPORTING INFORMATION

Additional supporting information may be found online in the Supporting Information section at the end of this article.

How to cite this article: Li Q, Li L, Yu M, et al. Elastomeric polyurethane porous film functionalized with gastrodin for peripheral nerve regeneration. *J Biomed Mater Res*. 2020;108: 1713–1725. https://doi.org/10.1002/jbm.a.36937